Bioorganic & Medicinal Chemistry Letters 19 (2009) 5140–5145

Contents lists available at ScienceDirect

Bioorganic & Medicinal Chemistry Letters

journal homepage: www.elsevier.com/locate/bmcl

Inhibitors of HIV-1 attachment. Part 4: A study of the effect of piperazine substitution patterns on antiviral potency in the context of indole-based derivatives ☆

Tao Wang [a,*], John F. Kadow [a], Zhongxing Zhang [a], Zhiwei Yin [a], Qi Gao [b], Dedong Wu [b], Dawn DiGiugno Parker [c], Zheng Yang [d], Lisa Zadjura [d], Brett A. Robinson [e], Yi-Fei Gong [e], Wade S. Blair [e], Pei-Yong Shi [e], Gregory Yamanaka [e], Pin-Fang Lin [e], Nicholas A. Meanwell [a]

[a] Department of Chemistry, Bristol-Myers Squibb Research and Development, 5 Research Parkway, Wallingford, CT 06492, United States
[b] Department of Analytical Research and Development, Bristol-Myers Squibb Research and Development, 5 Research Parkway, Wallingford, CT 06492, United States
[c] Department of Pharmaceutics, Bristol-Myers Squibb Research and Development, 5 Research Parkway, Wallingford, CT 06492, United States
[d] Department of Metabolism and Pharmacokinetics, Bristol-Myers Squibb Research and Development, 5 Research Parkway, Wallingford, CT 06492, United States
[e] Department of Virology, Bristol-Myers Squibb Research and Development, 5 Research Parkway, Wallingford, CT 06492, United States

ARTICLE INFO

Article history:
Received 5 June 2009
Revised 13 July 2009
Accepted 15 July 2009
Available online 18 July 2009

Keywords:
HIV
HIV attachment
gp120
Piperazine
$A^{1,3}$ strain

ABSTRACT

4-Fluoro- and 4-methoxy-1-(4-benzoylpiperazin-1-yl)-2-(1*H*-indol-3-yl)ethane-1,2-dione (**2** and **3**, respectively) have been characterized as potent inhibitors of HIV-1 attachment that interfere with the interaction of viral gp120 with the host cell receptor CD4. As part of an effort to understand fundamental aspects of this pharmacophore, discovered originally using a high throughput cell-based screen, modification and substitution of the piperazine ring was examined in the context of compounds **6a–ah**. The piperazine ring was shown to be a critical element of the HIV-1 attachment inhibiting pharmacophore, acting as a scaffold to deploy the indole glyoxamide and benzamide in a topographical relationship that complements the binding site on gp120.

The emergence of HIV-1 (human immunodeficiency virus-1) in 1981 foreshadowed an epidemic that has erupted to infect an estimated 40 million individuals worldwide with an annual death rate from progression to acquired immunodeficiency syndrome (AIDS) approaching three million.[1,2] The development of antiviral agents specifically targeting HIV has been a successful enterprise that has spawned 25 marketed drugs with two 'first-in-class' drugs, the integrase inhibitor raltegravir and the CCR5 antagonist maraviroc, approved by the FDA in 2008.[3] As might be anticipated with mechanistically novel drugs, raltegravir and maraviroc are not cross-resistant with existing anti-HIV therapeutics, providing important new agents for highly antiretroviral drug-experienced patients, many of whom harbor viruses expressing mutations conferring resistance to one or more of the major drug classes. The medical need for HIV-1 inhibitors acting by new mechanisms persists and it was against this backdrop that we developed and implemented a cell-based screening assay designed to identify lead molecules with novel modes of action.[4–8] 1-(4-Benzoylpiperazin-1-yl)-2-(1*H*-indol-3-yl)ethane-1,2-dione (**1**) emerged from that initiative as an inhibitor of HIV-1, representative of a series that was subsequently determined to interfere with the interaction between the membrane bound HIV glycoprotein 120 (gp120) and the CD4 receptor expressed on the membrane of human T cells and macrophages.[4–12] The engagement of CD4 by gp120 is the initial step in the process by which HIV-1 gains entry to the host cell cytosol where the replication process is initiated.

Indole **1** is a potent and specific inhibitor of HIV-1 in vitro that is not overtly cytotoxic toward a range of cell lines.[8] We have recently described structure–activity relationships associated with the substitutions patterns for both the indole heterocyclic core and the benzamide moiety.[13,14] Small substituents, including F, Cl, and MeO, at C-4 of the indole led to significant increases in potency while similar substituents introduced simultaneously at C-7 reinforced this effect, with a 4,7-disubstitution pattern clearly preferred.[13] Representative examples include indoles **2** and **3** which demonstrate EC_{50} values of 3 nM and 0.72 nM, respectively, in a pseudotype assay based on the HIV-1 LAI subtype, which compares with and EC_{50} of 86 nM for **1**.[8,13] In contrast, substitution of the benzamide moiety generally resulted in compounds with weaker antiviral activity although replacement by five-membered hetero-

☆ See Refs. 8, 13, and 14 for Parts 1–3 of this series.

* Corresponding author. Tel.: +1 203 677 6584; fax: +1 203 677 7702.
E-mail address: Tao.Wang@bms.com (T. Wang).

0960-894X/$ - see front matter © 2009 Elsevier Ltd. All rights reserved.
doi:10.1016/j.bmcl.2009.07.076

cycles was better tolerated.[14] With a basic understanding of two critical elements of the HIV-1 attachment inhibitor pharmacophore in hand, attention was directed towards probing the effect of structural variation of the piperazine moiety of **1**. In this Letter, we describe the results of that study which examined potential replacements for the piperazine and probed the effect of introducing both simple alkyl and more polar substituents on HIV-1 inhibitory activity. In addition, the effect of some of these changes on properties in assays conducted in vitro designed to predict aspects of pharmacokinetic performance in vivo was assessed.

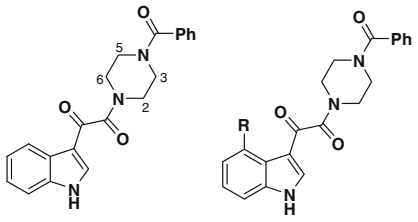

Several of the molecules targeted in this survey were prepared using the protocols outlined in Scheme 1. 4-Fluoro- or 4-methoxy-2-(1*H*-indol-3-yl)-2-oxoacetyl chloride (**4**), obtained from the corresponding acid by treatment with an excess of oxalyl chloride in Et_2O, was coupled with either a mono-benzoyl piperazine derivative **5** to afford target molecules **6** directly (Scheme 1, Route A) or a mono-Boc protected piperazine (**7**) (Scheme 1, Route B) using iPr_2NEt or Et_3N as the base in THF or CH_2Cl_2.[15] In the latter approach (Route B), the Boc group was removed under acidic conditions, typically by exposing to excess CF_3CO_2H acid in CH_2Cl_2, to provide the free amine **9** which was then acylated with benzoyl chloride to afford the final products **6**.

However, the use of Route A was dependent on the availability of mono-benzoylated piperazine derivatives **5** while Route B was restricted by the limited commercial availability of appropriately substituted mono-Boc piperazines **7**. In order to surmount these limitations, synthetic methodology was developed that allowed derivatization of substituted piperazines in a selective fashion. The mono-acylation of symmetrical diamines is typically complicated by the tendency for bis-acylation to occur,[15] a problem that was addressed by two complementary approaches that relied upon the selective activation[16] or deactivation[17] of one of the nitrogen atoms of piperazines **10**, as summarized in Scheme 2. The selective activation of one nitrogen atom in symmetrical piperazines **10** was accomplished by treatment with 2 equiv of *n*-BuLi in THF at room temperature followed by the addition of 1 equiv of benzoyl chloride, a protocol that furnished the mono-benzoyl derivatives **11** (Scheme 2).[16] In those cases where nitrogen deactivation was exploited, a symmetrical piperazine **10** was complexed with 9-BBN before the addition of benzoyl chloride, which reacted selectively with the remaining nitrogen atom to afford the target mono-substituted piperazines **11** (Scheme 2).[17]

When unsymmetrical piperazines were used as substrates, the lithium dianion typically reacted with benzoyl chloride to generate a mixture of the two isomers **13** and **14**, with low regioselectivity (Scheme 3, Route A).[15] Exceptions were *tert*-butyl- and 2,6-dimethyl-piperazine, for which benzoylation under these conditions occurred exclusively on the less hindered nitrogen. Unsymmetrical piperazines with alkyl, phenyl, and carboxylic acid-derived substituents could be selectively acyclated on the least hindered nitrogen atom with benzoyl chloride in CH_2Cl_2 without added base to afford **13** initially as the hydrochloride salt (Scheme 3, Route B).[18,19] A preparatively convenient strategy that avoided the complication of a mixture of products was developed for the benzoylation of some unsymmetrical piperazines **12** in which the more hindered nitrogen was derivatized selectively.[20] Exposure of the lithium dianion of an unsymmetrical piperazine **12** to triethylsilyl chloride protected the least hindered N atom in situ, allowing the more hindered N atom to be selectively acylated by benzoyl chloride to provide **14** (Scheme 3, Route C).[20]

Similar synthetic approaches were used to obtain a series of acyclic diamine derivatives that examined the effect of replacing the piperazine heterocycle with moieties that either conferred conformational relaxation or alternative constrained topologies, compounds (**1**–**9**) that are compiled in Table 1. The substituted piperazines **6a–ah** that constitute this survey are compiled in Table 2.

The antiviral properties of target compounds were assessed in a pseudotype virus infection system using an engineered virus.[4–10,13] A proviral clone of LAI virus in which the *env* gene is replaced by the firefly luciferase gene was co-transfected into HEK-293 cells with a plasmid expressing either a JRFL (CCR5-specific) or LAI (CXCR-4-specific) virus envelope. After 48 h, the supernatant containing the recombinant pseudovirus was harvested and the titer determined by performing serial dilutions in HeLa67 cells, which expresses the primary receptor CD4 and the HIV-1 coreceptors CXCR4 and CCR5. Virus growth was quantified by measuring luciferase activity (Luciferase Gene Reporter Assay Kit by Roche) 3 days post-infection. For the analysis of the antiviral activity of test

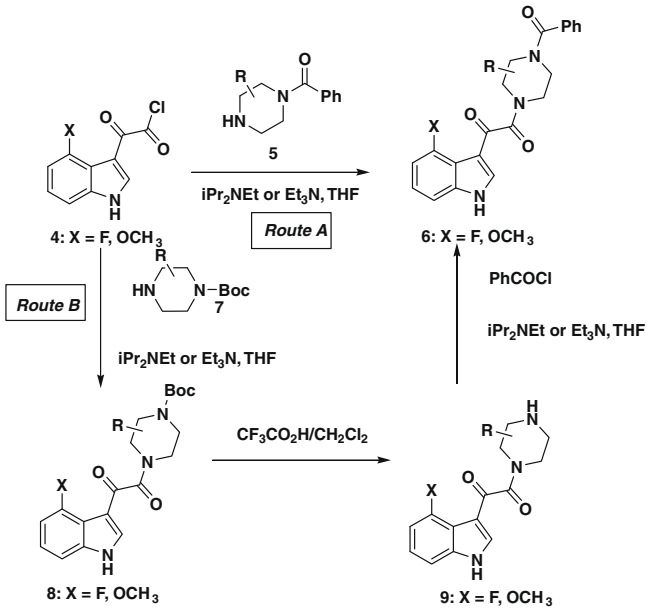

Scheme 1.

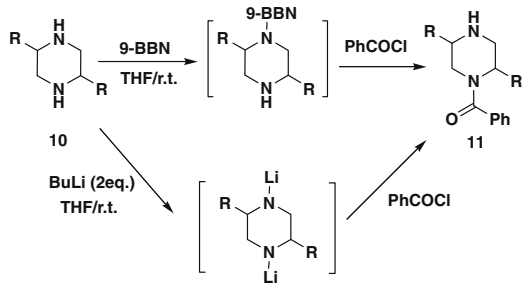

Scheme 2.

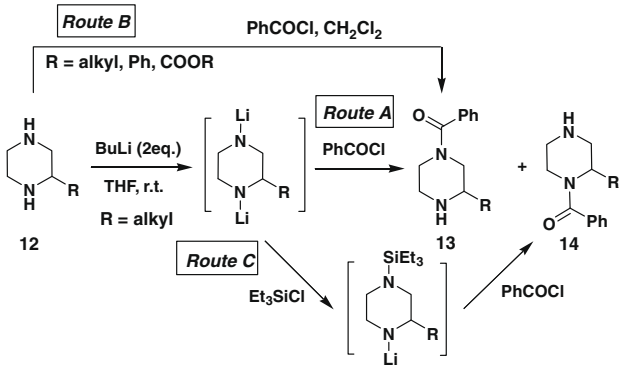

Scheme 3.

compounds, fourfold serial dilutions of compounds were added to pseudovirus-infected (containing either JRFL or LAI envelopes) HeLa67 cells at the time of infection. After 3 days, the extent of luciferase activity was compared to controls where no compound was added and the data used to calculate the EC_{50} values for individual compounds. The cytotoxicity of test compounds toward HeLa67 cells was determined in parallel using an XTT assay performed 3 days after compound addition. The results are presented in Tables 1 and 2 where individual results are provided as a measure of assay variability when the data reported are the average of two experiments.

The survey of potential piperazine replacements examined a series of simple alkylene linkers, either acyclic or cyclic, that explored a range of topologies. However, as summarized in Table 1, of these analogues only the *cis*-cyclohexane-1,2-diamine derivative (Table 1, entry 4) provided detectable antiviral activity and this compound is 10,000-fold weaker than the prototype **2**. These results are indicative of the importance of both the structural rigidity and precise topology conferred by the piperazine heterocycle, with the *cis*-cyclohexane-1,2-diamine presenting the closest approximation. The complementary survey summarized in Table 2 probes the effect of substitution of the piperazine ring on antiviral activity and correlates the structural changes with effects on metabolic stability in human and rat liver microsomes and permeability across a monolayer of Caco-2 cells grown to confluence. The introduction of a methyl group at C-2 of the piperazine ring, designated as the carbon atom proximal to the glyoxamide moiety, essentially preserved antiviral activity with a trend towards improved potency in the 4-F indole (**6a**) compared to the 4-methoxy congener (**6b**).

Table 1
Piperazine replacements

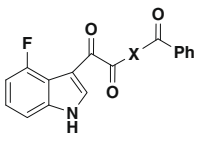

Entry no.	X	EC_{50} (μM) (JRFL)	CC_{50} (μM)
1	–NH–CH_2–CH_2–NH–	>50 (n = 1)	>300 (n = 1)
2	–N(CH_3)H–CH_2–CH_2–NH(CH_3)–	>50 (n = 1)	>300 (n = 1)
3	*trans*-Cyclohexane-1,2-diamine	>50 (n = 1)	>300 (n = 1)
4	*cis*-Cyclohexane-1,2-diamine	30.5 (25.5, 35.6)	65 (51, 79)
5	–NH–CH_2–CH_2–CH_2–NH–	>50 (n = 1)	>300 (n = 1)
6	–N(CH_3)H–CH_2–CH_2–CH_2NH(CH_3)–	>50 (n = 1)	>300 (n = 1)
7	Cyclohexane-1,3-diamine	>50 (n = 1)	>300 (n = 1)
8	1,4-Diazepane (homopiperazine)	>50 (n = 1)	>300 (n = 1)
9		>50 (n = 1)	>300 (n = 1)

Resolution of the enantiomers by chiral chromatography revealed some preference for the (*R*)-isomer in both series, more pronounced for the 4-fluoro-substituted pair of compounds **6c** and **6e**. However, progressive homologation of the methyl moiety to ethyl (**6g**) and *n*-propyl (**6h**) substituents was associated with an almost linear reduction in potency that fell substantially with the *n*-pentyl analogue **6i**. The effects of branching were even more detrimental, with the *iso*-propyl derivative **6j** determined to be 70-fold weaker than the ethyl derivative **6g** while the addition of a second methyl group to **6j** gave a compound with an EC_{50} above 5 μM, as examined with the *tert*-butyl derivative **6l**. Introducing branching remote from the piperazine core appeared to be better tolerated with **6k** only 10-fold less potent than **6g**. A comparable survey conducted at C-3 of the piperazine, compounds **6m**–**6s**, produced qualitatively similar results.

The effect of dual substitution with methyl groups was examined in the context of three compounds, **6t–6w**. The *cis*-C-2,C-6-dimethyl derivative **6t** exhibits comparable activity toward the LAI (CXCR4) envelope as the prototype **2** and the C-3 methyl derivative **6m** but is several fold weaker than the C-2 methyl derivative **6a**. Interestingly, **6t** exhibits reduced potency toward the CCR5-recognizing JRFL virus, indicative of some variation between the envelopes. The complementary topology, in which *cis*-disposed dimethyl substitution is deployed at C-3 and C-5 adjacent to the benzamide nitrogen atom of the piperazine, results in a compound **6u** that is 20-fold weaker than the mono-methyl compound **6m** toward both viral envelopes. The alternate C-2,C-5-dimethyl substitution afforded a very different pattern of antiviral activity, with the potency of the *trans*-disposed isomer **6v** markedly better than that of the *cis* isomer **6w**. In order to gain a deeper understanding of the effects of methyl substitution, particularly on piperazine ring conformation, single crystal X-ray structures were determined for compound **6u** and its debenzoylated precursor **9u**.[21] The solid state data indicate that the piperazine heterocycle in both molecules adopts a chair conformation but there are notable differences between the two compounds with respect to the disposition of the methyl groups, as depicted in Figure 1. For the unsubstituted NH derivative **9u**, the methyl substituents are equatorial while in the benzamide **6u** they adopt an axial configuration, establishing a strong 1,3-diaxial repulsive interaction estimated to be ~5.5 kcal/mol given the similarity between the dimethyl piperazine substructure of compound **6u** and 1,3-*cis*-dimethyl cyclohexane.[22] An alteration in configuration from an equatorial to axial disposition is a common observation for six-membered nitrogen-containing ring systems when the nitrogen adjacent to the carbon carrying the substituent is acylated.[23,24] This effect originates from the sp2 hybridization of the amide nitrogen[25] which constrains the carbonyl group of the amide to be coplanar with both carbons α-to the nitrogen atom. This leads to significant allylic 1,3 ($A^{1,3}$) strain[26,27] between the amide carbonyl moiety and the substituent installed at the carbon atom α-to the nitrogen atom.[28] In the case of **6u**, $A^{1,3}$ strain is relieved by both methyl groups adopting an axial configuration, which preserves the topographical relationship between the benzamide and glyoxamide elements inherent to **2**. However, since potency is eroded by 16-fold for the LAI virus and over 50-fold for the JRFL virus, these data suggest that the two axial methyl groups in this topographical relationship to the amide moieties are poorly tolerated by HIV-1 gp120. This phenomenon also provides a potential explanation for the large difference in antiviral potency observed between compounds **6v** and **6w**. For compound **6v**, the *trans*-relationship allows the two methyl groups to adopt an axial disposition without altering the preferred chair conformation of the piperazine ring,[29,30] leading to the retention of biological activity, EC_{50} = 4.72 nM against the LAI subtype although the JRFL envelope is again more sensitive to structural changes. However, for the *cis*-dimethyl derivative **6w**, the pipera-

Table 2
Substituted piperazines

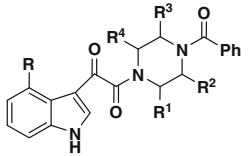

Compd no.	R	R^1	R^2	R^3	R^4	EC_{50} (nM)	CC_{50} (μM)	HLM% rem at 10 min	RLM% rem at 10 min	Caco-2 (nm/s)	*c* log *P*
2	F	H	H	H	H	2.9 (LAI) 2.4 (JRFL)	>300	98	51	47	2.43
3	OCH_3	H	H	H	H	0.72 (0.87, 0.57) (LAI)	>300 (n = 2)	100	88	43	2.23
6a	F	CH_3	H	H	H	0.56 (0.53, 0.57) (LAI) 0.37 n = 5 (JRFL)	>300 (n = 2)	82	12	72	2.95
6b	OCH_3	CH_3	H	H	H	1.57 (1.78, 1.37) (LAI)	>300 (n = 2)	84	72	N/A	2.75
6c	F	(*R*)-CH_3	H	H	H	<0.16 (LAI) 0.42 (0.43, 0.41) (JRFL)	>300 (n = 2)	74	2	54	2.95
6d	OCH_3	(*R*)-CH_3	H	H	H	0.93 (0.91, 0.96) (LAI) 0.58 (0.86, 0.30) (JRFL)	>300 (n = 3)	84	56	46	2.75
6e	F	(*S*)-CH_3	H	H	H	1.38 (1.54, 1.23) (LAI) 1.58 (2.13, 1.03) (JRFL)	>300 (n = 2)	85	32	88	2.95
6f	OCH_3	(*S*)-CH_3	H	H	H	3.33 (2.67, 3.99) (LAI) 0.58 (0.75, 0.42) (JRFL)	>300 (n = 3)	98	75	N/A	2.75
6g	F	CH_3CH_2	H	H	H	7.10 (5.73, 8.47) (LAI)	157 (154, 159)	55	8	150	3.48
6h	F	$CH_3CH_2CH_2$	H	H	H	15.4 (14.0, 16.9) (LAI)	94 (81, 107)	52	11	172	4.01
6i	F	$CH_3(CH_2)_4$	H	H	H	855 (1316, 394) (LAI)	33 (33, 34)	29	0	154	5.06
6j	F	$(CH_3)_2CH$	H	H	H	471 (510, 432) (LAI)	90 (85, 95)	59	31	165	3.88
6k	F	$(CH_3)_2CHCH_2$	H	H	H	79.2 (104.3, 54.1) (LAI)	28 (27, 30)	38	7	171	4.40
6l	F	$(CH_3)_3C$	H	H	H	>5000 (n = 2) (LAI)	105 (98, 112)	68	49	170	4.27
6m	F	H	CH_3	H	H	2.60 (3.38, 1.83) (LAI) 2.14 (2.12, 2.16) (JRFL)	>300 (n = 2)	100	32	36	2.95
6n	F	H	CH_3CH_2	H	H	5.38 (6.21, 4.54) (LAI)	188 (183, 193)	63	25	171	3.48
6o	F	H	$CH_3CH_2CH_2$	H	H	3.55 (3.55, 3.56) (LAI)	100 (97, 103)	50	25	154	4.01
6p	F	H	$CH_3(CH_2)_4$	H	H	>5000 (n = 2) (LAI)	45 (43, 47)	45	3	69	5.06
6q	F	H	$(CH_3)_2CH$	H	H	23.3 (16.7, 30.0) (LAI)	130 (127, 135)	63	39	161	3.88
6r	F	H	$(CH_3)_2CHCH_2$	H	H	303 (280, 326) (LAI)	69 (69, 69)	35	13	190	4.40
6s	F	H	$(CH_3)_3C$	H	H	>5000 (n = 2) (LAI)	127 (127, 127)	58	44	190	4.27
6t	F	CH_3	H	H	*cis*-CH_3	3.3 (0.97, 6.33) (LAI) 23.7 (JRFL)	206 (131, 281)	55	2	<15	3.47
6u	F	H	CH_3	*cis*-CH_3	H	48.4 (18.7, 102.1) (LAI) 125 (80, 169) (JRFL)	200 ± 53 (n = 4)	69	16	73	3.47
6v	F	CH_3	H	*trans*-CH_3	H	4.7 (3.90, 5.53) (LAI) 23.1 (15.4, 27.8) (JRFL)	102 ± 56 (n = 4)	43	0	50	3.47
6w	F	CH_3	H	*cis*-CH_3	H	676 (650, 702) (LAI)	>300 (n = 2)	76	59	96	3.47
6x	F	Ph	H	H	H	>5000 (n = 2) (LAI)	28 (27, 30)				
6y	F	H	Ph	H	H	3400 (2933, 3875) (LAI)	109 (103, 116)				
6z	F	(*S*)-$PhCH_2$	H	H	H	>5000 (n = 2) (LAI)	47 (46, 47)				
6aa	F	H	(*S*)-$PhCH_2$	F	F	>500 (n = 2) (LAI)	>100 (n = 2)				
6ab	F	$CONH_2$	H	H	H	>5000 (n = 2) (LAI)	>300 (n = 2)				
6ac	F	H	$CONH_2$	H	H	>500 (n = 2) (LAI)	>300 (n = 2)				
6ad	F	(*S*)-CO_2CH_3	H	H	H	>5000 (n = 2) (LAI)	207 (191, 223)				
6ae	F	H	(*S*)-CO_2CH_3	H	H	3.1 (2.10, 4.03) (LAI)	>300 (n = 2)				
6af	F	$CO_2CH_2CH_3$	H	H	H	>5000 (n = 2) (LAI)	128 (127, 128)				
6ag	F	CO_2H	H	H	H	>5000 (n = 2) (LAI) 836 (398, 1275) (JRFL)	>300 (n = 4)				
6ah	F	CH_2OH	H	H	H	640 (467, 814) (JRFL)	>300 (n = 2)				

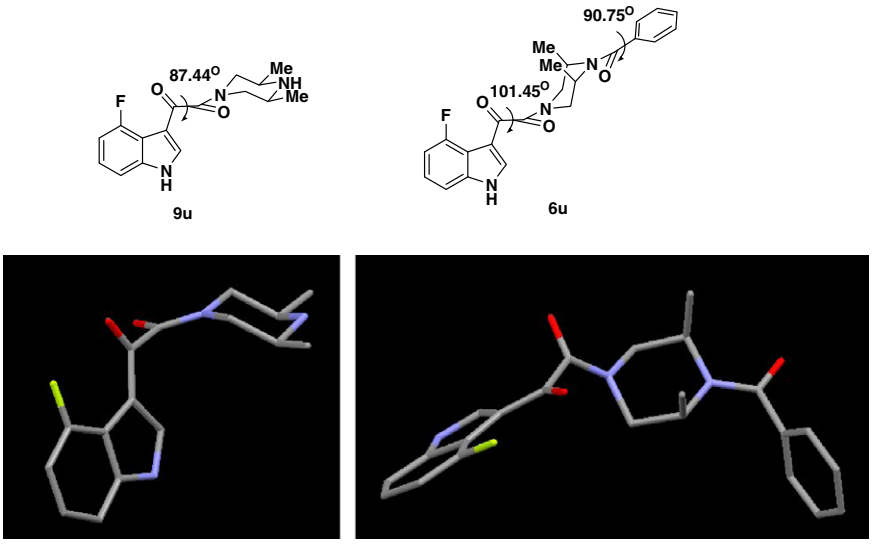

Figure 1.

zine ring is unable to adopt a chair conformation that avoids $A^{1,3}$ strain between one of the methyl groups and either the proximal benzamide or glyoxylamide carbonyl moiety. This compels the heterocyclic ring to distort from the idealized chair conformation in an attempt to position the two methyl groups in pseudo-axial orientations if it is to effectively preserve amide resonance.[31,32] The resulting deformation of the topographical projections of the amide moieties is presumably responsible for the large reduction in potency observed with **6w** towards the LAI strain envelope, EC_{50} = 676 nM. Reinforcing the importance of the relative disposition of the two amide moieties, both the homopiperazine and the 2,5-diazabicyclo[2.2.1]heptane derivatives, with the latter constrained to a boat conformation, are inactive (Table 1, entries 8 and 9, respectively). Collectively, these data suggest that the chair conformation of the piperazine ring is essential for optimal HIV-1 attachment inhibition and that there is limited tolerance for substitution of the piperazine ring, with a single methyl group deployed at C-2 that adopts an axial disposition preserving or enhancing antiviral activity.[33]

The final aspect of this survey examined a range of larger substituents that encompassed the potential to establish hydrogen bonding and π–π interactions, probed with compounds **6x**–**6ah**. These substituents produced uniformly weak inhibitors of HIV-1 attachment with the exception of the ester **6ae** which performed comparably to the prototype **2**.

The effect of these structural modifications on metabolic stability and membrane permeability revealed interesting trends with all compounds examined exhibiting reduced stability in rat liver microsomes compared to human liver microsomes, a profile inherent to 4-fluoro prototype **2**.[8] In general, liver microsomal stability was inversely related to lipophilicity, which increased in concert with the size of the substituents explored. Not surprisingly, membrane permeability increased in parallel with enhanced lipophilicity, as estimated by *c* log *P* values (Table 2), with several compounds achieving permeability coefficients of >100 nm/s, predictive of good intestinal permeability based on comparison to standards. However, none of these compounds provided a combination of potency, metabolic stability, and membrane permeability that would qualify for a more detailed examination of the pharmacokinetic properties in vivo.

In summary, the piperazine ring in this series of HIV-1 attachment inhibitor is of critical importance as a scaffold to deploy the benzamide and indole glyoxamide moieties, the key pharmacophoric elements, in a topographical relationship that complements the binding site of gp120.[34,35] An examination of substitution patterns has illuminated fundamental aspects of the SAR and conformational preferences. The incorporation of a simple methyl substituent to the piperazine ring proximal to the glyoxamide offers some advantage and this element was incorporated into BMS-378806 (**15**), a compound that was evaluated clinically. However, BMS-378806 (**15**) failed to achieve targeted plasma exposure levels[36] and antiviral efficacy in HIV-1-infected subjects was subsequently demonstrated with an optimized analogue, BMS-488043 (**16**).[36] Nevertheless, BMS-378806 (**15**) protected macaque monkeys against a vaginally administered challenge with simian-human immunodeficiency virus (SHIV) when administered topically.[37]

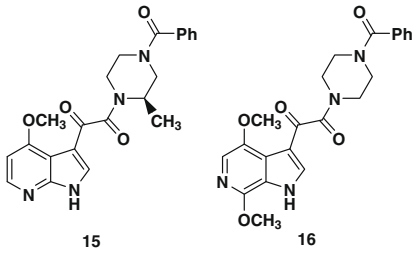

References and notes

1. Pomerantz, R. J.; Horn, D. L. *Nat. Med.* **2003**, *9*, 867.
2. Merson, M. H. *New Eng. J. Med.* **2006**, *354*, 2414.
3. De Clercq, E. *Int. J. Antimicrob. Agents* **2009**, *33*, 307.
4. Blair, W. S.; Spicer, T. P. World Patent Application, WO-2001/96610, December 20th, 2001.
5. Blair, W. S.; Deshpande, M.; Fang, H.; Lin, P-F.; Spicer, T. P.; Wallace, O. B.; Wang, H.; Wang, T.; Zhang, Z.; Yeung, K.-S. World Patent Application, WO2000/76521, December 21st, 2000.
6. Lin, P.-F.; Blair, W. S.; Wang, T.; Spicer, T. P.; Guo, Q.; Zhou, N.; Gong, Y.-F.; Wang, H.-W. H.; Rose, R.; Yamanaka, G.; Robinson, B.; Li, C.-B.; Fridell, R.; Deminie, C.; Demers, G.; Yang, Z.; Zadjura, L.; Meanwell, N. A.; Colonno, R. J. *Proc. Natl. Acad. Sci. U.S.A.* **2003**, *100*, 11013.
7. Wang, H.-W. H.; Williams, R. E.; Lin, P.-F. *Curr. Pharm. Des.* **2004**, *10*, 1785.
8. Wang, T.; Zhang, Z.; Wallace, O. B.; Deshpande, M.; Fang, H.; Yang, Z.; Zadjura, L. M.; Tweedie, D. L.; Huang, S.; Zhao, F.; Ranadive, S.; Robinson, B.; Gong, Y.-F.; Riccardi, K.; Spicer, T. P.; Deminie, C.; Rose, R.; Wang, H.-W. H.; Blair, W. S.; Shi, P.-Y.; Lin, P.-F.; Colonno, R. J.; Meanwell, N. A. *J. Med. Chem.* **2003**, *46*, 4236.
9. Guo, Q.; Ho, H.-T.; Dicker, I.; Fan, L.; Zhou, N.; Friborg, J.; Wang, T.; McAuliffe, B. V.; Wang, H.-W. H.; Rose, R. E.; Fang, H.; Scarnati, H. T.; Langley, D. R.; Meanwell, N. A.; Abraham, R.; Colonno, R. J.; Lin, P.-F. *J. Virol.* **2003**, *77*, 10528.
10. Ho, H.-T.; Nowicka-Sans, B.; McAuliffe, B.; Li, C.-B.; Yamanaka, G.; Zhou, N.; Fang, H.; Dicker, I.; Dalterio, R.; Gong, Y.-F.; Wang, T.; Yin, Z.; Ueda, Y.;

Matiskella, J.; Kadow, J. F.; Clapham, P.; Robinson, J.; Colonno, R.; Lin, P.-F. *J. Virol.* **2006**, *80*, 4017.
11. Si, Z.; Madani, N.; Cox, J. M.; Chruma, J. J.; Klein, J. C.; Schön, A.; Phan, N.; Wang, L.; Biorn, A. C.; Cocklin, S.; Freire Chaiken, I.; E.; Smith, A. B., III; Sodroski, J. G. *Proc. Natl. Acad. Sci. U.S.A.* **2004**, *101*, 5036.
12. Madani, N.; Perdigoto, A. L.; Srinivasan, K.; Cox, J. M.; Chruma, J. J.; LaLonde, J.; Head, M.; Smith, A. B., III; Sodroski, J. G. *J. Virol.* **2004**, *78*, 3742.
13. Meanwell, N. A.; Wallace, O. B.; Fang, H.; Wang, H.; Deshpande, M.; Wang, T.; Yin, Z.; Zhang, Z.; Pearce, B. C.; James, J.; Yeung, K.-S.; Qiu, Z.; Wright, J. J. K.; Yang, Z.; Zadjura, L.; Tweedie, D. L.; Yeola, S.; Zhao, F.; Ranadive, S.; Robinson, B. A.; Gong, Y.-F.; Wang, H.-G. H.; Blair, W. S.; Shi, P.-Y.; Colonno, R. J.; Lin, P.-F. *Bioorg. Med. Chem. Lett.* **2009**, *19*, 1977.
14. Meanwell, N. A.; Wallace, O. B.; Wang, H.; Deshpande, M.; Pearce, B. C.; Trehan, A.; Yeung, K.-S.; Qiu, Z.; Wright, J. J. K.; Robinson, B. A.; Gong, Y.-F.; Wang, H.-W. G.; Blair, W. S.; Shi, P.-Y.; Lin, P.-F. *Bioorg. Med. Chem. Lett.* **2009**, *19*, 5136.
15. Bender, J. A.; Meanwell, N. A.; Wang, T. *Tetrahedron* **2002**, *58*, 3111.
16. Wang, T.; Zhang, Z.; Meanwell, N. A. *J. Org. Chem.* **1999**, *64*, 7661.
17. Zhang, Z.; Yin, Z.; Kadow, J. F.; Meanwell, N. A.; Wang, T. *Org. Lett.* **2003**, *5*, 3399.
18. Rossen, K.; Weissman, S. A.; Sager, J.; Reamer, R. A.; Askin, D.; Volante, R. P.; Reider, P. J. *Tetrahedron Lett.* **1995**, *36*, 6419.
19. Fukushi, H.; Mabuchi, H.; Terashita, Z.-I.; Nishikawa, K.; Sugihara, H. *Chem. Pharm. Bull.* **1994**, *42*, 551.
20. Wang, T.; Zhang, Z.; Meanwell, N. A. *J. Org. Chem.* **2000**, *65*, 4740.
21. Diffraction data were collected at room temperature using a Bruker SMART 2K CCD diffractometer equipped with graphite-monochromated Cu Kα radiation (λ = 1.54056 Å) or a Kappa-CCD diffractometer equipped with graphite-monochromated Mo Kα radiation (λ = 0.71073 Å). An empirical absorption correction utilized the SADABS routine (Bruker AXS. 1998, SMART and SAINTPLUS. Area Detector Control and Integration Software, Bruker AXS, Madison, Wisconsin, USA). The unit cell parameters were determined using the entire data set. The structures were solved by direct methods and refined by the full-matrix, least-squares techniques, using the SHELXTL software package (Sheldrick, GM. 1997, SHELXTL. Structure Determination Programs. Version 5.10, Bruker AXS, Madison, Wisconsin, USA.). Non-hydrogen atoms were refined with anisotropic thermal displacement parameters. Hydrogen atoms involved in hydrogen bonding were located in the final difference Fourier maps, while the positions of the other hydrogen atoms were calculated from an idealized geometry with standard bond lengths and angles. They were assigned isotropic temperature factors and included in structure factor calculations with fixed parameters. Crystal data for **6u**: colorless plate crystals grown from ethyl acetate are a hemi-EtOAc solvate, Orthorhombic, space group $P2_12_12_1$, a = 6.3659(1) Å, b = 16.7942(4) Å, c = 21.7178(6) Å, $\alpha = \beta = \gamma = 90°$, V = 2321.85(9) Å^3, Z = 4, d_x = 1.292 g cm^{-3}, 12936 reflections measured, 3988 independent reflections (R_{int} = 0.0297), 273 parameters refined with 3197 reflections ($I \geq 2\sigma$, $R(F^2)$ = 0.0496, $wR(F^2)$ = 0.1398, S = 1.071, $w = 1/[\sigma^2 (F_o^2) + (0.094\ P)^2 + 0.088\ P]$ where $P = (F_o^2 + 2\ F_c^2)/3$, $-0.161 \leq \Delta\rho \leq 0.148$ e/Å^3. Crystal data for **9u**: colorless prism crystals grown from CH_2Cl_2/EtOAc are a mono-hydrate, Monoclinic, space group $P2_1/c$, a = 8.7886(1) Å, b = 12.2014(2) Å, c = 15.5672(3) Å, β = 98.449(1), V = 1651.20(5) Å^3, Z = 4, d_x = 1.293 g cm^{-3}, 14,606 reflections measured, 2739 independent reflections (R_{int} = 0.0254), 225 parameters refined with 2246 reflections ($I \geq 2\sigma$, $R(F^2)$ = 0.0377, $wR(F^2)$ = 0.0984, S = 1.017, $w = 1/[\sigma^2 (F_o^2) + (0.050\ P)^2 + 0.425\ P]$ where $P = (F_o^2 + 2\ F_c^2)/3$, $-0.155 \leq \Delta\rho \leq 0.160$ e/Å^3. Full crystallographic data have been deposited to the Cambridge Crystallographic Data Center (reference numbers: CCDC 738923 (**6u**) and CCDC 738924 (**9u**)). Copies of the data can be obtained free of charge via the internet at http://www.ccdc.cam.ac.uk.
22. Nasipuri, D. *Stereochemistry of Organic Compounds: Principles and Applications*. Wiley Eastern Limited: New Delhi, India, 1991.
23. Brameld, K. A.; Kuhn, B.; Reuter, D. C.; Stahl, M. *J. Chem. Inf. Model.* **2008**, *48*, 1.
24. Bruno, I. J.; Cole, J. C.; Edgington, P. R.; Kessler, M.; Macrae, C. F.; McCabe, P.; Pearson, J.; Taylor, R. *Acta Crystallogr., Sect. B* **2002**, *58*, 389.
25. Andrews, P. R.; Munro, S. L. A.; Sadek, M.; Wong, M. G. *J. Chem. Soc., Perkin Trans. 2* **1988**, 711.
26. Johnson, F.; Malhotra, S. K. *J. Am. Chem. Soc.* **1965**, *87*, 5492.
27. Johnson, F. *Chem. Rev.* **1968**, *68*, 375.
28. Chevallier, F.; Beaudet, I.; Grognec, E. L.; Toupet, L.; Quintard, J.-P. *Tetrahedron Lett.* **2004**, *45*, 761.
29. Lepore, U.; Gains, P.; Bombieri, G.; Gilli, G.; Montaudo, G. *Cryst. Struc. Commun.* **1977**, *6*, 7.
30. Okamoto, K.; Sekido, K.; Itoh, J.; Noguchi, T.; Hirokawa, S. *Bull. Chem. Soc. Jpn.* **1979**, *52*, 1896.
31. Sakurai, T.; Nakamaru, M.; Tsuboyama, S.; Tsuboyama, K. *Acta Crystallogr., Sect. B* **1977**, *33*, 3568.
32. Hiramatsu, H.; Sakurai, T.; Tsuboyama, S.; Tsuboyama, K. *Acta Crystallogr., Sect. B* **1978**, *34*, 3469.
33. Lu, R.-J.; Tucker, J. A.; Zinevitch, T.; Kirichenko, O.; Konoplev, V.; Kuznetsova, S.; Sviridov, S.; Pickens, J.; Tandel, T.; Brahmachary, E.; Yang, Y.; Wang, J.; Freel, S.; Fisher, S.; Sullivan, A.; Zhou, J.; Stanfield-Oakley, S.; Greenberg, M.; Bolognesi, D.; Bray, B.; Koszalka, B.; Jeffs, P.; Khasanov, A.; Ma, Y.-A.; Jeffries, C.; Liu, C.; Proskurina, T.; Zhu, T.; Chucholowski, A.; Li, R.; Sexton, C. *J. Med. Chem.* **2007**, *50*, 6535.
34. Kong, R.; Tan, J. J.; Ma, X. H.; Chen, W. Z.; Wang, C. X. *Biochim. Biophys. Acta* **2006**, *1764*, 766.
35. Teixeira, C.; Serradji, N.; Maurel, F.; Barbault, F. *Eur. J. Med. Chem.*, *in press.*. doi:10.1016/j.ejmech.2009.03.028.
36. Hanna, G.; Lalezari, J.; Hellinger, J.; Wohl, D.; Masterson, T.; Fiske, W.; Kadow, J. F.; Lin, P-F.; Giordano, M.; Colonno, R. J.; Grasela D. *Abstract 141*, 11th Conf. Retroviruses Opportunistic Infections, San Francisco, Feb 8–11, 2004.
37. Veazey, R. S.; Klasse, P. J.; Schadr, S. M.; Hu, Q.; Ketas, T. J.; Lu, M.; Marx, P. A.; Dufour, J.; Colonno, R. J.; Shattock, R. J.; Springer, M. S.; Moore, J. P. *Nature* **2005**, *438*, 99.